Multiphysics Numerical Simulation of the Transient Process in Electrochemical Machining

Yuanlong CHEN, Xiang LI, Jinyang LIU, Yichi ZHANG
School of Mechanical Engineering, Hefei University of Technology, Hefei, 230009, Anhui, China,
E-mails: chenyualong@hfut.ede.cn; lix1117@163.com; ljyhfut@163.com; zyc346121469@163.com

1. Introduction

Titanium alloy materials have been used to make turbine blades for engines with high temperature resistance, low density, and high strength [1]. Electrochemical machining meets the machining needs of turbine blades [2]. It have the advantages of no loss of tool cathode, no machining deformation and internal stress on the surface of the workpiece [3]. However, electrochemical machining involves electric field, flow field, temperature field, etc. The change of one factor will cause the common changes of other physical fields, making it difficult to accurately predict the electrochemical machining process [4]. Many scholars have used experiments and simulations to understand electrochemical coupling and processing mechanisms.

Yao et al. [5] simulated the electrolyte flow rate and pressure distribution in different tubular electrodes of electrochemical machining, and obtained better hole machining results without sparks and short circuits. Chai et al. [6] analyzed the influence of the flow field distribution in the inter-electrode gap on the machining accuracy and stability of the cooling holes of the blade. Liu et al. [7] studied the surface quality of titanium alloy processed by electrochemical jet. Simulations and experiments have found that the voltage is 24 V, the gap between electrodes is 0.6 mm, the electrolyte flow rate is 2.1 L·min-1 and the nozzle travel speed is 25 μm·s-1, which can obtain good processing quality. Patro et al. [8] predicted the evolution of the anode shape of the workpiece in electrochemical machining based on the finite element method. Zhou et al. [9] established a multi-field coupling model to simulate the influence of hydrogen bubbles near the cathode and low-speed electrolyte on heat transfer during electrochemical machining. Chandrasekhar et al. [10] used the Entropy-VIKOR method to study the influence of the relevant parameters of microporous electrochemical machining on the material removal rate and overcutting.

To sum up, although there have been a large number of literatures on electrochemical machining simulations and experiments, they have not really coupled the electric field-flow field-temperature field-structure field. Most researchers simulating electrochemical processing actually do not really consider the coupling effect between multiple physical fields comprehensively, either presupposing that the electrochemical processing reaches an equilibrium state or ignoring the effect of hydrogen and not considering the effect of deformation of geometry on the coupling. Therefore, in this paper, various factors have been comprehensively considered to establish a coupling model involving electric-flow-temperature-structure field.

The established multi-physics coupling model is used to study the temperature, hydrogen volume fraction, electrolyte conductivity, current density and workpiece profile change curve of the electrochemical machining blade profile at different machining times.

2. Multi-physics coupling simulation model establishment

Electrochemical machining is a process method based on the principle of anode dissolution to remove material in the form of ions with the aid of the cathode [11]. The tool cathode is connected to the negative electrode, and the workpiece anode is connected to the positive electrode. There is a certain machining gap between the cathode and the anode to allow the electrolyte to flow through the machining gap at high speed. The flowing electrolyte is not only used as a conductive medium, but also can take away the electrolytic products in electrochemical processing [12]. The processing principle is shown in Fig. 1.
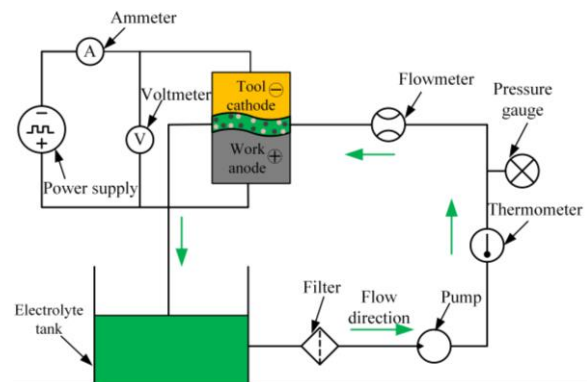

Fig. 1 Principle of electrochemical machining ECM

In order to obtain high-quality workpieces, electrochemical machining needs to meet the following conditions [13]:

a) the machining gap between anode and cathode is small, usually between 0.1-1mm;

b) the electrolyte needs to be updated in time to wash away the electrochemical reaction products and play a certain role in cooling;

c) the current density on the anode metal workpiece is high, between 10-100A/cm^2.

Electrochemical machining involves multi-physics coupling, including electric field, flow field, temperature field and structure field. The relationship between the physical fields is shown in Fig. 2.
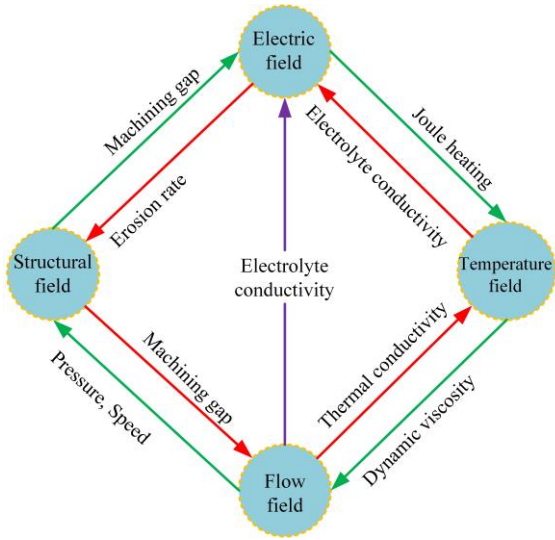
Fig. 2 Multi-physics coupling relationship of electrochemical machining

Each physics field influences each other. The change of a variable will cause various physical fields to change, which makes it difficult to accurately predict the electrochemical machining process. Finite element software has been widely used as decoupling software. Not only can it more intuitively predict the entire machining process, but also can optimize the parameters to provide more reasonable machining parameters for the final electrochemical machining experiment. The multi-physics coupling simulation steps are shown in Fig. 3.
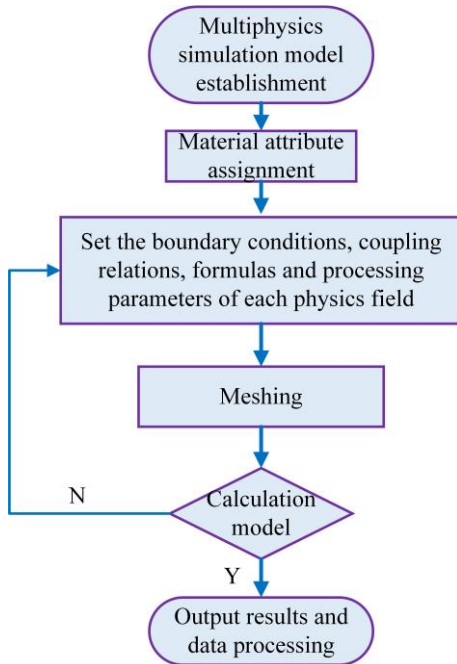

Fig. 3 Multi-field coupling simulation steps

In the software, corrosion, primary current, bubble flow, $k\sim\varepsilon$ model, fluid heat transfers and deformation geometry modules are selected to simulate the current density, hydrogen volume fraction, electrolyte conductivity, temperature and anode erosion changes in the machining gap. Comprehensive consideration of various influencing factors to simplify the model into two dimensions, as shown in Fig. 4 (I represents tool cathode; II represents the fluid region; III represents the workpiece anode; *1, 2, 8* and

9 represent the boundaries of the tool cathode; *4, 5, 6* and *10* represent the boundaries of the workpiece anode; *7* represents the electrolyte inlet boundary;*3* represents the electrolyte outlet boundary).
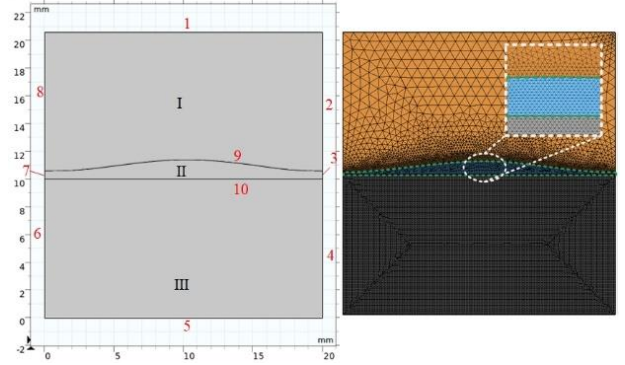

Fig. 4 Two-dimensional model and meshing

The current module, bubbly flow, $k\sim\varepsilon$ module and fluid heat transfer module are selected, the transient state is used as a research for related simulations. In the electric field module, it is assumed that the electrochemical machining process has entered the equilibrium machining state and the electric field parameters do not change with time. Meanwhile, assuming that the conductivity of the electrolyte remains constant and isotropic, the current efficiency of the electrolyte is approximately constant. According to the basic theory of electric field, the distribution of electric field potential Φ in the entire processing area (referring to the processing gap in the text) conforms to Laplace equation [14]:

$$\frac{\partial^2 \phi}{\partial x^2} + \frac{\partial^2 \phi}{\partial y^2} = 0 . \tag{1}$$

In the turbulent bubble flow module, it is assumed that the gas produced by electrolysis obeys the ideal gas state equation and the current efficiency of the electrolyte is approximately constant. The relationship between electrolyte conductivity k, electrolyte temperature T and bubble rate β is summarized as the following formula [15]:

$$k = k_0[1 + \alpha(T_1 - T_0)][1 - \beta]^n , \tag{2}$$

where: k_0 represents the initial conductivity of the electrolyte; α represents the temperature coefficient of conductivity, and the value is generally 0.02~2; T_0 represents the initial temperature of the electrolyte; n is the influence index of bubble rate on conductivity and the value is generally 1.5~2. It can be seen from formula (2) that the increase in temperature and hydrogen volume fraction will cause the conductivity to decrease.

In electrochemical machining, hydrogen mainly precipitates on the surface of the cathode. According to Faraday's law, the amount of hydrogen produced per unit time and per unit area on the surface of the cathode tool can be obtained [16]:

$$N_{H2} = \frac{\eta i M}{2F} , \tag{3}$$

where: i is the current density; F is the Faraday constant; η is the current efficiency; M is the molar mass of hydrogen.

In the flow heat transfer module, the temperature of the electrolyte in the machining gap is affected by the interaction of the electric field and the flow field, which satisfies the convection-diffusion equation [17]:

$$\rho c_p \frac{\partial T}{\partial t} + \rho c_p v_1 \cdot \nabla T = \nabla \cdot (k \nabla T) + Q , \qquad (4)$$

where: c_p is the specific heat capacity of the electrolyte; Q is the heat generated during processing. The heat generated in the electrochemical machining mainly comes from two aspects: Joule heat generated by the current in the machining gap and heat generated by the electrode reaction (the heat generated is very small and can be ignored). In the simulation, the settings of boundary conditions and material properties are very important and have a significant impact on the results, and the relevant settings are shown in Tables 1 and 2, respectively.

Table 1

Boundary conditions in the interface for the boundaries numbered in Fig. 2

Physical field	Boundary condition	
Electric field	$\Gamma_2=U_1=16$ V	$\Gamma_1=U_0=0$
	$\Gamma_{2,4,6,8}=0$ (insulating boundaries)	$\Gamma_{3,7}\approx0$ (free boundaries)
Flow field	$\Gamma_3=P_1=0.6$, MPa	$\Gamma_4=P_0=0$, MPa
	$k_1=k_0\cdot(1-\beta)^2\cdot[1+0.02\,(T-T_0)]$	$k_0=7.2$ S/m, $T_0=293$ K
	$\Gamma_5=2i\cdot(2\cdot F)^{-1}$	$F=96500$, A·s·mol^{-1}
Temperature field	$\Gamma_3=T$	$\Gamma_{1,2}=T_0$
Structural field	$\Gamma_{1,2,9,7,8}=0.5$, mm·s^{-1}	

Table 2

Simulation material parameters

Type	Parameter	Value
Electrolyte (NaNO$_3$)	Initial conductivity, S/m	7.2
	Initial temperature, K	293
	Density, Kg·m^{-})	1070
	Specific heat capacity, J·(kg·K)$^{-1}$	3730
Titanium alloy (Ti6Al4V)	Density, Kg·m^{-3}	4430
	Specific heat capacity, J·(kg·K)$^{-1}$	611
	Volume electrochemical equivalent, cm^3·(A·min)$^{-1}$	0.0017

3. Analysis of simulation results

In electrochemical machining, temperature and hydrogen volume affect the distribution of electrical conductivity, and the distribution of electrical conductivity will affect the current density, thereby affecting the erosion process of anode materials.

3.1. Temperature in the processing gap at different times

The main source of heat in electrochemical machining is the Joule heat generated by the current in the machining gap. It can be seen from the temperature change cloud diagram in Figure 5 that when processing 100 s, the reaction time is short and the distance between cathode and anode is large, which makes the temperature difference between processing gaps not large. With the increase of processing time, the increase of current density and electrochemical reaction degree generates more Joule heat,

which leads to a gradual increase in temperature.

However, during processing, the products of the anode corrosion and the temperature are carried by the flowing electrolyte from the inlet to the outlet along the flow direction and accumulate at the outlet, which will cause the temperature near the outlet to be higher. Therefore, the temperature gradually increases along the process direction, and the temperature change trend at different times is shown in Fig. 6.
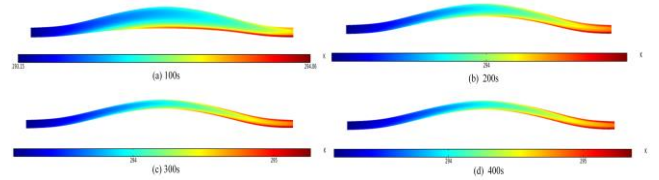

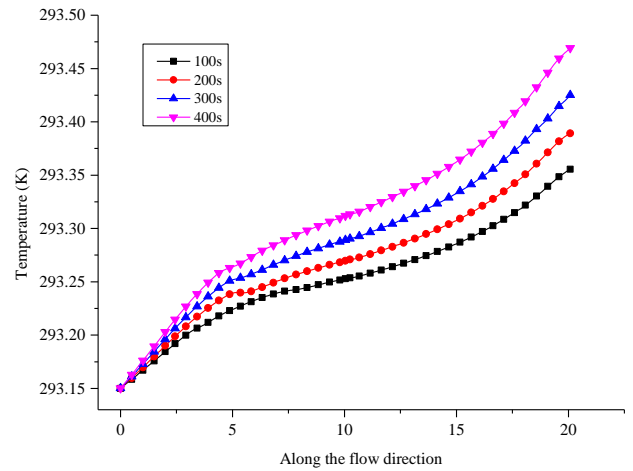Fig. 5 Cloud diagram of temperature changes at different times

Fig. 6 Temperature change curve along the process direction

3.2. Hydrogen volume fraction in the processing gap at different times

Fig. 7 is a hydrogen volume cloud diagram at different times. It can be seen from the figure that at the beginning of processing, the tool cathode is far from the workpiece anode and only a slight degree of electrochemical reaction occurs at the anolyte interface, the reduction reaction at the cathode produces less hydrogen. With the increase of processing time, the content of hydrogen at the outlet gradually increases, reaching the maximum with a hydrogen content of about 14% when the processing time is greater than 300s. Although there is almost no hydrogen at the inlet, the hydrogen content continues to increase along the process direction and reaches the maximum at the outlet, as shown in Fig. 8.

Analysis can be considered that in electrochemical machining, the cathode is continuously fed to the anode, the current density gradually increases and the degree of electrochemical reaction (redox reaction) of the anode surface material is gradually enhanced and hydrogen is precipitated while the anode surface material is removed. The electrolyte at the entrance is updated in time, the electrolysis products and hydrogen in the process are taken away by the flowing electrolyte, finally accumulate at the exit, which causes the hydrogen content to gradually increase along the process direction.
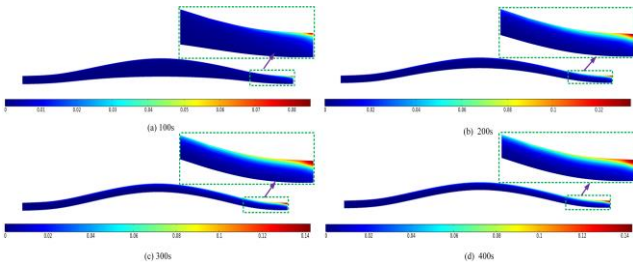
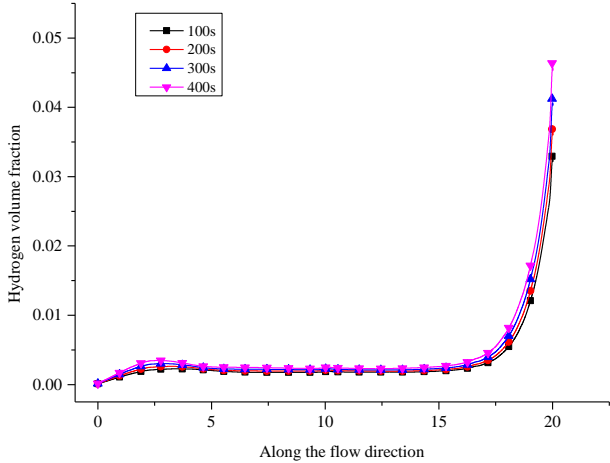Fig. 7 Cloud diagram of hydrogen volume change at different times

Fig. 8 Hydrogen volume change curve along the process direction

3.3. Electrolyte conductivity in the machining gap at different times

Fig. 9 is a cloud diagram of electrolyte conductivity changes at different times. It can be seen that the electrical conductivity distribution is relatively uniform in the initial stage of processing. The electrical conductivity gradually decreases with the increase of processing time. The analysis believes that as the processing progresses, the current density increases and the electrochemical reaction is violent, which not only generates more Joule heat and reaction heat, but also the hydrogen ions in the electrolyte get electrons at the cathode to undergo a reduction reaction to generate hydrogen. Temperature and hydrogen have a comprehensive effect on the electrical conductivity distribution.
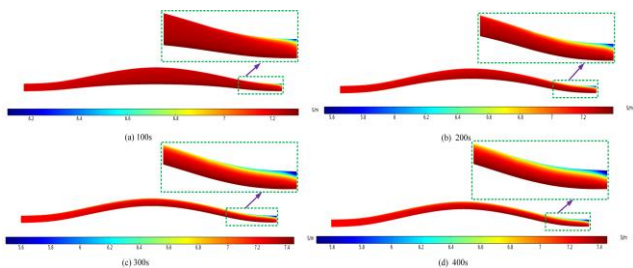

Fig. 9 Cloud diagram of electrolyte conductivity change at different times

It can also be seen from Figure 10 that the conductivity gradually decreases along the flow direction. This is because the electrolyte at the entrance is updated in time and the content of hydrogen is low, so the conductivity is relatively high. Combining Figs. 5, 7 and formula (2), it can be seen that along the process direction, the gradual

increase in hydrogen content and temperature will reduce the conductivity of the electrolyte.
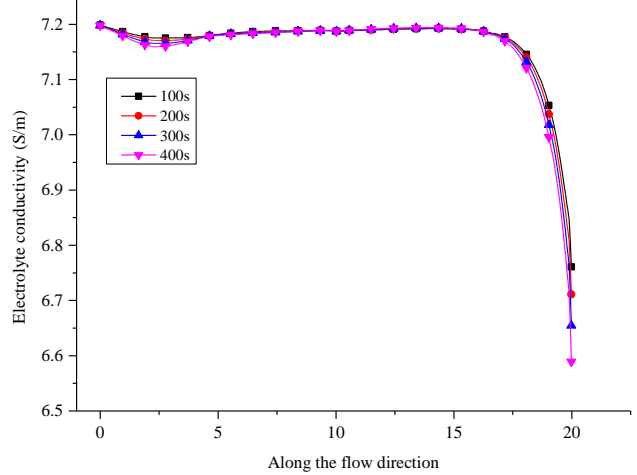

Fig. 10 Current density variation curve along the process direction

3.4. Current density in the machining gap at different times

It can be seen from Fig. 11 that the current density is low in the middle and high on the two sides. Along the process 0-10 mm and 10-20 mm, the cathode tool is close to the anode surface, so the current density is high. At 10mm, the cathode tool is the farthest away from the anode surface, so the current density is small. It can also be seen from the current density change curve in Fig. 12 that the current density at the entrance is greater than the current density at the exit.
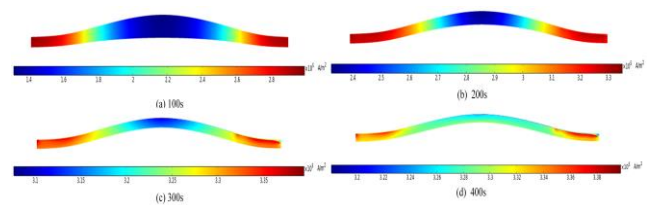

Fig. 11 Cloud diagram of current density changes at different times
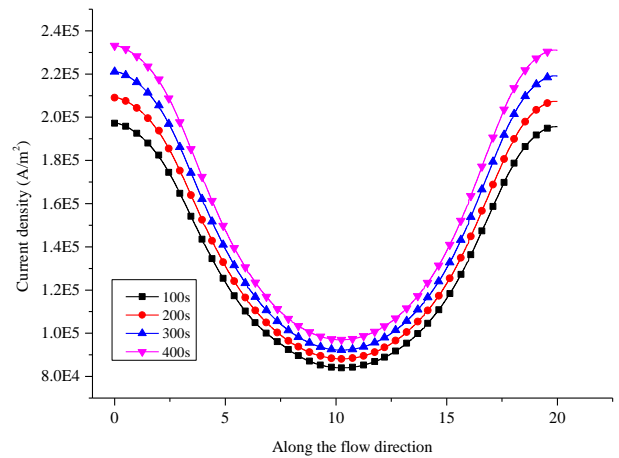

Fig. 12 Current density variation curve along the process direction

It is believed that during the electrochemical machining process, the surface of the metal anode material is continuously oxidized and eroded away, the hydrogen at-

oms of the tool cathode get electrons to undergo a reduction reaction, hydrogen gas is released. The flowing electrolyte will bring hydrogen, temperature and electrolysis products to accumulate near the outlet. The electrical conductivity will be affected by hydrogen and temperature, so the higher the hydrogen content at the outlet, the lower the electrolyte conductivity and the current density.

3.5. Shape of anode material changes at different times

It can be seen from Fig. 13 that as the processing time increases, the cathode continues to feed to the anode, the current density gradually increases and the anode material is gradually removed. When the processing time reaches 300 s, the anode has basically been processed into the shape of the cathode. As the processing time continues to increase, the material continues to be eroded. The middle part of the cathode is far from the anode surface and the two sides are closer to the anode surface, so the current density in the middle area is less than the current density on the two sides, which causes the erosion of the intermediate material to be less than the erosion of the materials on both sides.

Combining Figs. 5, 7, 9 and 11 can be analyzed: the electrolyte is updated at the inlet in time, the electrolysis product, hydrogen and temperature are brought to the outlet by the flowing electrolyte. The conductivity and current density are large, which makes the material quickly removed. However, the accumulation of hydrogen and temperature at the outlet leads to lower conductivity and current density and the amount of material erosion is relatively small, so the erosion trend of the material is parabolic as shown in Fig. 14.
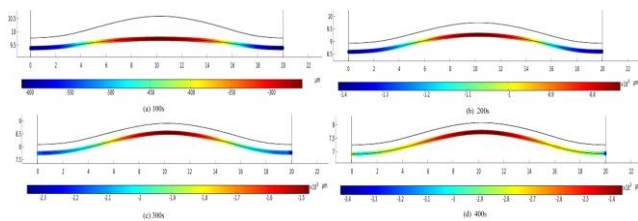

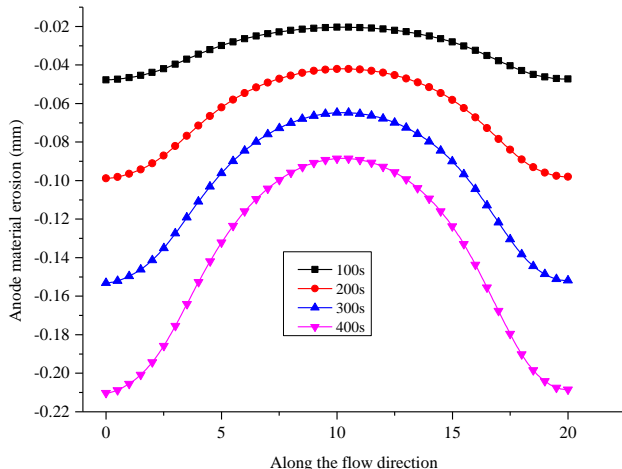Fig. 13 Cloud diagram of workpiece shape change at different moments

Fig. 14 Change curve of workpiece profile along the process direction

4. Conclusions

Electrochemical machining is a processing method in which anode metal is continuously dissolved and finally formed. By simulating the current density, hydrogen content, conductivity, temperature and anode material removal in the processing gap at different moments during the electrochemical processing, this gives a better understanding of the variation of each physical field and allows to correct the cathode structure based on the simulation results.

1. Temperature and bubbles comprehensively affect the electrical conductivity distribution. The electrolyte flowing in the machining gap will bring temperature and hydrogen to the outlet and accumulate there, and the conductivity will gradually decrease.

2. Along the flow direction, the current density and the anode material erosion rate are parabolic with upper and lower openings, respectively. The electrolyte at the entrance is updated in a timely manner and the higher current density will result in a faster material erosion rate. In the middle, the initial machining gap is larger and the current density is smaller, so the material erosion is slower. Although the processed products, hydrogen and temperature are accumulated at the outlet, the current density and material erosion rate are lower than those at the inlet, but still greater than at the middle position.

The current density, hydrogen volume fraction, electrolyte conductivity, temperature and workpiece shape changes in the processing area at different processing times are simulated to help understand the changes in the physical fields at different times during the electrochemical machining process and provide a better guidance for actual processing. At the same time, it can also design the cathode shape reasonably according to the simulation results and provide a theoretical basis for the selection of actual electrochemical machining parameters.

References

1. **Karpenko, O.; Oterkus, S.; Oterkus, E.** 2021. Peridynamic investigation of the effect of porosity on fatigue nucleation for additively manufactured titanium alloy Ti6Al4V, Theoretical and Applied Fracture Mechanics 112:102925.
http://dx.doi.org/10.1016/j.tafmec.2021.102925.

2. **Xu, J.; Zhu, D.; Lin J.;** et al. 2020. Flow field design and experimental investigation of electrochemical trepanning of diffuser with a special structure, International Journal of Advanced Manufacturing Technology 107(1): 1551-1558.
http://dx.doi.org/10.1007/s00170-020-05091-6.

3. **Selvarajan, L.; Sasikumar, R.; Mohan, D.G.;** et al. 2020. Investigations on electrochemical machining (ECM) of Al7075 material using copper electrode for improving geometrical tolerance, Materials Today, Proceedings 27(3): 2708-2712.
http://dx.doi.org/10.1016/j.matpr.2019.12.188.

4. **Morgunov, Y. A.; Petukhov, S. L.; Saushkin, B. P.** 2021. Micro-ECM of the aerodynamic surface understating, Solid State Phenomena 316: 214-220.
http://dx.doi.org/10.4028/www.scientific.net/SSP.316.214.

5. **Yao, J.; Nie, Y. J.; Chen, Z. T.** 2017. Design and

analysis of flow field in electrochemical cutting processing by arranged tube electrode, Applied Mechanics & Materials 872:67-76.
http://dx.doi.org/10.4028/www.scientific.net/AMM.872.67.

6. **Chai, M.; Li, Z.; Yan, H.;** et al. 2019. Experimental investigations on aircraft blade cooling holes and CFD fluid analysis in electrochemical machining, Advances in Materials Science and Engineering 2019(6):1-11.
http://dx.doi.org/10.1155/2019/4219323.

7. **Liu, W.; Luo, Z.; Li,Y.;** et al. 2019. Investigation on parametric effects on groove profile generated on ti1023 titanium alloy by jet electrochemical machining, International Journal of Advanced Manufacturing Technology 100(9-12): 2357-2370.
http://dx.doi.org/10.1007/s00170-018-2804-1.

8. **Patro, S.K.; Mishra, D.K.; Arab, J.;** et al. 2020. Numerical and experimental analysis of high-aspect-ratio micro-tool electrode fabrication using controlled electrochemical machining, Journal of Applied Electrochemistry 50(2): 169-184.
http://dx.doi.org/10.1007/s10800-019-01380-5.

9. **Zhou, X. C.; Cao, C. Y.; Wang, H. X.;** et al. 2020. Study on the multi-field coupling model of electrolyte temperature distribution in electrochemical machining, International Journal of Advanced Manufacturing Technology 109(5-6): 1-8.
http://dx.doi.org/10.1007/s00170-020-05775-z.

10. **Chandrasekhar, S.; Prasad, N.** 2020. Multi-response optimization of electrochemical machining parameters in the micro-drilling of AA6061-TiB 2 in situ composites using the entropy–vikor method, Proceedings of the Institution of Mechanical Engineers Part B Journal of Engineering Manufacture 234(10): 1311-1322.
http://dx.doi.org/10.1177/0954405420911539.

11. **Wang, J.; Xu, Z.; Wang, J.;** et al. 2021. Electrochemical machining on blisk channels with a variable feed rate mode, Chinese Journal of Aeronautics 34(6): 151-161.
http://dx.doi.org/10.1016/j.cja.2020.08.002.

12. **Lohrengel, M. M.; Rataj, K. P.; Münninghoff, T.** 2016. Electrochemical machining-mechanisms of anodic dissolution, Electrochim Acta 201: 348-353.
http://dx.doi.org/10.1016/j.electacta.2015.12.219

13. **Lohrengel, M. M.; Rataj, K. P.; Münninghoff, T.** 2016. Electrochemical machining-mechanisms of anodic dissolution, Electrochim Acta 201: 348-353.
http://dx.doi.org/10.1016/j.electacta.2015.12.219

14. **Wu, M.; Liu, J. W.; He, J. F.;** et al. 2020. Fabrication of surface microstructures by mask electrolyte jet machining, International Journal of Advanced Manufacturing Technology 148:103471.
http://dx.doi.org/10.1016/j.ijmachtools.2019.103471.

15. **Liu, G. D.; Tong, H.; Li, Y.;** et al. 2020. Multiphysics research on electrochemical machining of micro holes with internal features, International Journal of Advanced Manufacturing Technology 110(5-6): 1527-1542.
http://dx.doi.org/10.1007/s00170-020-05973-9.

16. **Hackert, M.; Paul, R.; Kowalick, M.;** et al. 2017. Characterization of an electrochemical machining process for precise internal geometries by multiphysics simulation, Procedia Cirp 58: 175-180.
http://dx.doi.org/10.1016/j.procir.2017.04.021.

17. **Chen, Y. L.; Fang, M.; Jiang, L. J.** 2017. Multiphysics simulation of the material removal process in pulse electrochemical machining (PECM), International Journal of Advanced Manufacturing Technology 91(5-8): 2455-2464.
http://dx.doi.org/10.1007/s00170-016-9899-z.

Y. L. Chen, X. Li, J. Y. Liu, Y. C. Zhang

MULTIPHYSICS NUMERICAL SIMULATION OF THE TRANSIENT PROCESS IN ELECTROCHEMICAL MACHINING BLADE PROFILE

S u m m a r y

To fully understand the electrochemical machining profile, a multi-physics coupling simulation model including flow-electric-temperature-structure field were established to analyze the corrosion process of the anode material and the change trend of temperature, hydrogen volume fraction, electrolyte conductivity and current density in the processing gap. The analysis results show that the temperature and hydrogen content gradually increase along the process direction. The current density and material removal showed a parabolic trend of the upper opening and the lower opening, respectively. The simulation of the different physical field changes in the electrochemical machining blade profile can not only better understand the complex physical phenomena in the machining, but also provide a theoretical basis for the selection of actual electrochemical machining parameters.